Journal of Thermal Analysis and Calorimetry (2019) 138:1–10
https://doi.org/10.1007/s10973-019-08209-5

Insight into the catalytic thermal decomposition mechanism of ammonium perchlorate

TG-MS study using cotton-assisted hydrothermally synthesized nano copper oxide catalyst

Deepthi L. Sivadas[1] · Deepthi Thomas[1] · M. S. Haseena[1] · T. Jayalatha[1] · G. Rekha Krishnan[1] · Salu Jacob[1] · R. Rajeev[1]

Received: 18 July 2018 / Accepted: 22 March 2019 / Published online: 5 April 2019

Abstract

Copper oxide (CuO) is an attractive burn rate modifier for composite solid propellant based on ammonium perchlorate (AP). However, the mechanism of catalytic decomposition of AP in the presence of CuO is still uncertain. Amount of gaseous products at various decomposition temperatures of AP in the presence and absence of CuO is lacking. Herein, a systematic study using thermogravimetry-mass spectroscopy (TG-MS) was carried out to evaluate the effect of CuO on AP decomposition mechanism. A novel hydrothermal method was reported for the preparation of nanosized copper oxide. The conversion of precursor $Cu(NO_3)_2{\cdot}3H_2O$ to intermediate $Cu_2(NO_3)(OH)_3$ was accomplished by in situ carbonization of small quantity of cotton fiber in the hydrothermal reaction chamber. pH of the reaction medium was controlled by utilizing the nitric acid in the reaction medium by in situ carbonization of cotton. This synthetic method aimed to minimize the shape-controlling agents and strong alkali for controlling the pH of the reaction medium for the preparation of catalyst grade CuO. Evolved gas analysis of AP decomposition products by TG-MS showed increased oxygen, chlorine and nitrogen evolution and decreased ammonia evolution in the presence of CuO, compared with that of AP without catalyst. This confirmed the enhanced interaction of ammonia and perchloric acid; the initial decomposition products of AP; and their further reaction in the presence of CuO. The change in composition of volatile products indicates change in mechanism of AP decomposition from proton transfer to electron transfer in the presence of CuO.

Electronic supplementary material The online version of this article (https://doi.org/10.1007/s10973-019-08209-5) contains supplementary material, which is available to authorized users.

✉ Deepthi L. Sivadas
deepthisivadas@gmail.com

[1] Analytical and Spectroscopy Division, Vikram Sarabhai Space Centre, Thiruvananthapuram 695 022, India

Graphical abstract

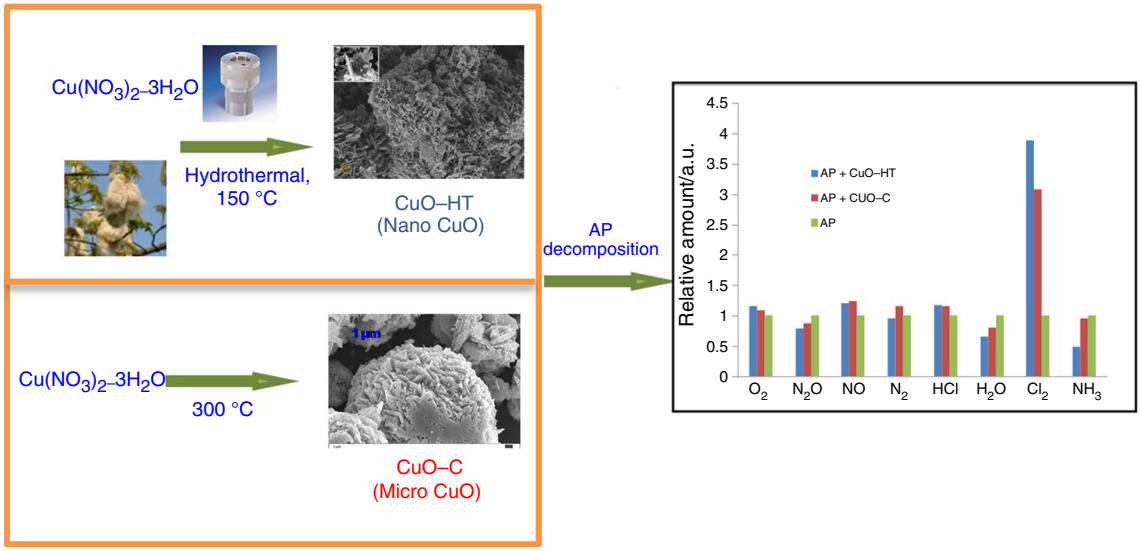

Keywords Copper oxide · Hydrothermal · Ammonium perchlorate · Burn rate modifier · TG-MS

Introduction

In the field of composite solid propellants for various rocket motors, a continuing desire exists to increase the burning rate. For increasing the burn rate of propellant, either the rate of decomposition of AP or combustion of fuels must be increased. This can be achieved by reducing the particle size of ammonium perchlorate (AP) or the metallic fuel (e.g., aluminum) or by incorporating reactive species in the polymer binder or by the addition of a burn rate modifier (BRM) like copper chromite, copper oxide, ferric oxide [1–5]. A burn rate modifier can alter the burning rate of propellant by increasing the rate of decomposition of AP as well as by accelerating the combustion of fuel without affecting the visco-elastic properties [6, 7]. Good compatibility with propellant ingredients, better consistency and reproducibility in propellant burn rate make copper oxide a better burn rate modifier in composite solid propellants. It has been reported that copper (II) oxide can significantly increase the heat released during the decomposition of catalyzed AP with respect to pure AP [8–10]. Catalytic activity of CuO can be increased by increasing the surface area, thereby increasing the number of active sites and effective contact between catalyst and reactant. Thus, nanosized copper oxide with low particle size and high surface area is ideal choice as BRM. However, the positive role of copper oxide on the thermal decomposition mechanism of AP lacks solid evidence, in terms of the comparative fraction of gas evolved at the decomposition temperature of AP in the absence and presence of CuO catalyst. The catalytic activity depends on the purity, number of active sites, surface area, textural property, etc. Therefore, it is important to understand the catalytic mechanism of CuO particles of different textural property and active sites. Most importantly, the catalyst should be free of the contaminations from external reagents, used for controlling the pH and particle size during the synthesis.

Over the last two decades, enormous scientific interest has been gathered in realizing morphology-controlled nanometal oxides for catalyst application. CuO with different morphologies, viz, nanosheets, nanorods, nanowires, nanoparticle, has been reported [11–14]. These morphologies have been achieved by various synthetic methods like wet chemical, hydrothermal, thermal decomposition, physical and chemical vapor deposition [15, 16]. Selection of suitable method is critical in obtaining CuO particles of desired properties for specific applications. Most of the reported works on the synthesis of CuO nanostructures made use of shape-controlling agents, capping agents or ultra-dilution of the precursors for controlling the growth and dimensions of the nanoparticles [15]. However, challenges exist in the complete removal of the shape-controlling reagents from the products. External reagents may depreciate the active surface area and porosity, which are the desired properties of catalysts. It is also observed that

temperature and pH of the reaction medium significantly affected the morphology of CuO obtained [17–19]. Slight variation in the pH may result in multiple products, viz, copper hydroxide, copper hydroxyl nitrate, CuO. Hence, it is highly desirable to design chemical methods which do not require size-controlling agents or ultra-dilution or stringent control of pH for the synthesis of nanostructures.

In the present work, a modified hydrothermal method was adopted for the preparation of morphology-controlled CuO nanostructures using natural cotton as pH-controlling agent for the first time. The conversion of precursor $Cu(NO_3)_2{\cdot}3H_2O$ to $Cu_2(OH)_3NO_3$ intermediate was accomplished by in situ carbonization of cotton in a hydrothermal chamber followed by decomposition at 300 °C to yield nanosized CuO. Well-dispersed and uniformly oriented CuO nanostructures were obtained at relatively lower temperatures. The prepared CuO particles were expected to have single phase, uniform morphology, more active sites, the absence of external reagent, etc., a promising candidate to study the role of catalyst in AP decomposition mechanism. For better understanding the role of hydrothermal synthesis for controlling the morphology and functional properties, CuO was also prepared by direct decomposition of $Cu(NO_3)_2{\cdot}3H_2O$ at 300 °C. The prepared CuO particles were evaluated for chemical and structural properties.

Catalytic activity of the prepared CuO on the thermal decomposition of AP was studied in detail using TG-MS technique to acquire clear evidence of the AP decomposition mechanism. This was done by quantifying and comparing the gas evolution from AP at different temperatures, in the presence of CuO particles with size range of micro- and nanoscale.

Experimental

Materials and methods

All chemicals (analytical reagent grade) were purchased from Merck India Pvt. Ltd and used without further purification. Deionized water was used in all the experiments. Raw cotton fibers were collected from cotton tree (Bombax pentandrum Linn-Gossypium arboretumin) at VSSC Campus, Thiruvananthapuram, India. Ammonium perchlorate manufactured in VSSC was used for catalytic activity evaluation studies.

Hydrothermal synthesis of CuO (CuO-HT)

Hydrothermal synthesis of copper oxide was performed in a typical Teflon-lined stainless steel autoclave. A mixture of 1.0 g of $Cu(NO_3)_2{\cdot}3H_2O$ and trace quantity of cotton [2 mass% of $Cu(NO_3)_2{\cdot}3H_2O$] was mixed with 10 mL of deionized water and sealed in the Teflon-lined steel autoclave. The reaction chamber was kept in an oven maintained at temperature of 150 °C for 8 h. After the reaction, the autoclave was cooled to room temperature. Light blue-colored solid formed was filtered, washed with water and dried in vacuum at 100 °C for 4 h. The solid was calcined at 300 °C in air atmosphere for 3 h to produce black copper oxide powder (CuO-HT). Control experiments were also carried out in the absence of cotton to study the role of cotton in the reaction.

Combustion synthesis of CuO (CuO–C)

CuO was also synthesized by the combustion of $Cu(NO_3)_2{\cdot}3H_2O$ at 300 °C in air for 3 h.

Instrumental characterization

FT-IR spectra of the samples were obtained on a PerkinElmer Spectrum GX-A FT-IR spectrometer in the 4000–400 cm^{-1} wave number range. The crystal phases of the prepared products were identified by Bruker D8-discover X-ray diffraction spectrometer using Cu Kα radiation (1.5418 A°) at a scan rate of 2.5° min^{-1}. Particle size of CuO samples was determined by nanoparticle size analyzer (Malvern Model: Nano Zen 3601). Samples were dispersed in ethylene glycol prior to the analysis. SEM pictures were taken by a Carl Zeiss, Supra 55 Model Field Emission Scanning Electron Microscope to evaluate the shape and size of the synthesized products. Gold film was deposited on the surface of the samples to improve the conductivity. Surface area of copper oxide particles was measured by a Quantachrome NOVA 1200E surface area analyzer. The samples were degassed at 250 °C for 4 h prior to analysis. The specific surface area was measured from the isotherm in the relative pressure range between 0.05 and 0.2, according to the Brunauer–Emmett–Teller (BET) method. Simultaneous TG-DSC (TA Instruments Q600) was employed for evaluating the effect of prepared copper oxide particles on the thermal decomposition of ammonium perchlorate. In thermal analysis experiments, a sample mass of 10 ± 1 mg in platinum sample cup was used at a heating rate of 5 °C min^{-1} and 99.99% pure nitrogen was purged through the thermobalance at a flow rate of 100 mL min^{-1}. For the evaluation of catalytic activity of synthesized copper oxide samples, fine AP (average particle, 50 μm) was thoroughly mixed with CuO powders in the mass ratio 99.7:0.3 and subjected to thermal decomposition studies using TG-DSC techniques. PerkinElmer Pyris 1 TGA thermogravimetric analyzer clubbed with a PerkinElmer Clarus SQ8T mass spectrometer was used for the TG-MS study of evolved gas.

Results and discussion

Hydrothermal method has been frequently adopted for the preparation of nanostructured CuO with different crystallinity, morphology and self-assembly. In all hydrothermal reactions, alkali (urea, NaOH, etc.) is added to the metal salt while loading to hydrothermal reaction chamber. A number of reaction, viz, formation of $Cu_2(OH)_3NO_3$ and/or $Cu(OH)_2$ and finally CuO with respect to the change in pH of the solution, occur during hydrothermal process [20]. pH and temperature control are very critical, since multiple product formation may affect the property of copper oxide catalyst.

The present hydrothermal synthesis is designed to minimize the by-products by avoiding the use of alkali for changing the pH of solution. A small quantity of cotton (2 mass% of copper salt) was added to the aqueous acidic solution of copper nitrate to indirectly control the pH of the solution. At 150 °C, carbonization of cotton initiated due to high pressure and temperature experienced in the autoclave. Carbonization of cotton was accelerated by the nitric acid formed from copper nitrate salt solution. Thus, carbonization of cotton indirectly increased the pH of reaction medium to neutral by consuming nitric acid. This condition further accelerates the decomposition of copper nitrate inside the autoclave and converts the nitrate to $Cu_2(NO_3)(OH)_3$. The precipitation of copper hydroxyl nitrate ($Cu_2(NO_3)(OH)_3$) involves the reaction of hydroxyl ion with copper nitrate. Trace amount of carbonized cotton in the product was removed by the calcinations of resultant solid in air atmosphere at 300 °C, whereas $Cu_2(NO_3)(OH)_3$ was converted to cupric oxide (CuO-HT). Conversion of $Cu_2(NO_3)(OH)_3$ to cupric oxide (CuO-HT) involves dehydroxylation followed by decomposition of nitrate anions by releasing structural water and nitrogen dioxide.

Analysis of intermediate $Cu_2(NO_3)(OH)_3$

The intermediate of hydrothermal reaction was subjected to XRD and FT-IR analysis for structural information and TG analysis for selecting the decomposition temperature for its conversion to CuO. XRD pattern of light blue product obtained after hydrothermal reaction is shown in Fig. 1a confirmed the structure of intermediate as $Cu_2(OH)_3NO_3$ (copper(II) hydroxy nitrate) (PDF 00-045-0594).

Figure 1b shows the FT-IR spectrum of $Cu_2(NO_3)(OH)_3$. IR absorptions are basically due to hydroxyl and nitrate groups. Signals in the range 3300–3600 cm^{-1} correspond to the –OH groups. The Cu–O–H bonds give rise to bending absorptions at different frequencies 819 and 675 cm^{-1}. Signals at 1046, 819, 1362, 1384, 1420 cm^{-1} correspond to infrared absorptions of nitrate groups.

The intermediate product $Cu_2(NO_3)(OH)_3$ was subjected to TG analysis, and the resulting curve is given in Fig. 2. It can be seen that the decomposition of $Cu_2(NO_3)(OH)_3$ starts at 200 °C and completes before 300 °C. Hence, 300 °C was fixed as the calcinations temperature of $Cu_2(NO_3)(OH)_3$ to prepare CuO.

Analysis of CuO

FT-IR spectrum of the calcined product Cu(II)O (CuO-HT) shows (Fig. 3) an absorption band is in the region 480–610 cm^{-1} which is attributed to Cu(II)O. The peaks at

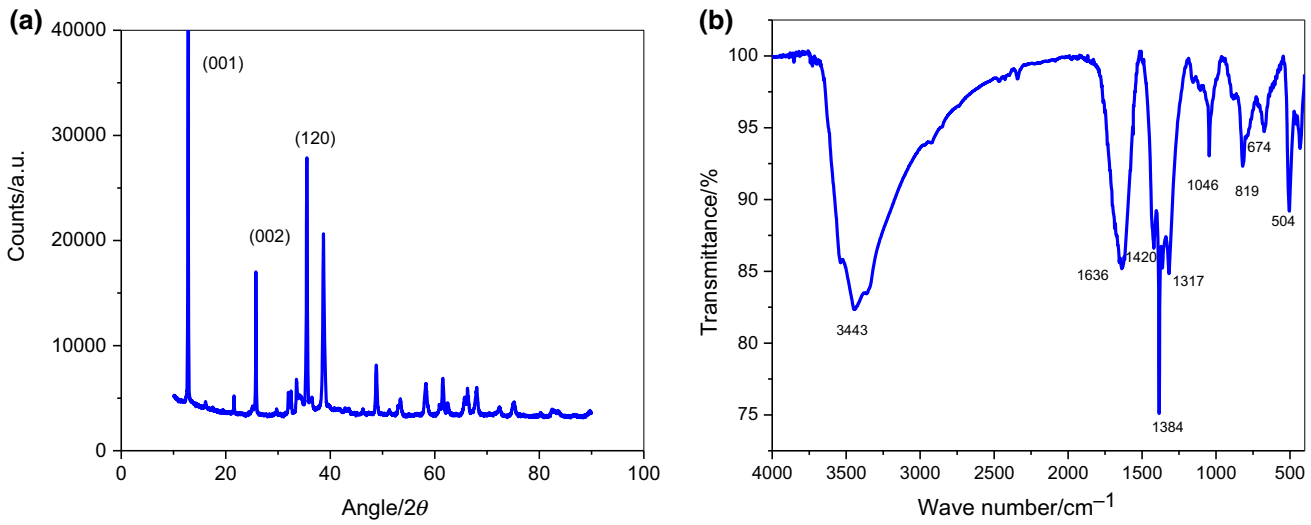

Fig. 1 **a** XRD pattern and **b** FT-IR spectrum of $Cu_2(OH)_3NO_3$

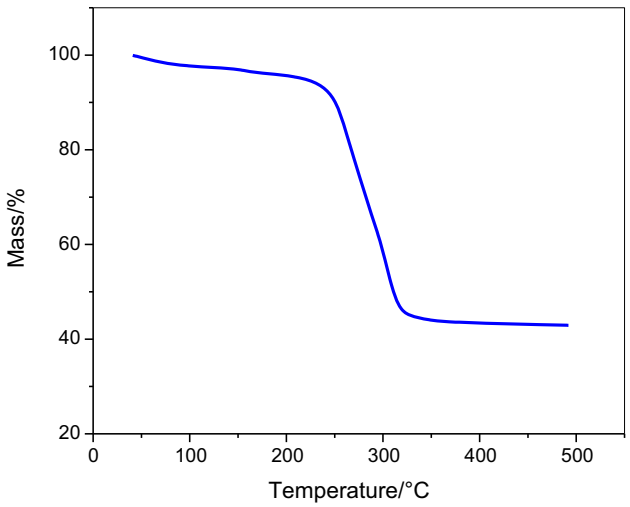

Fig. 2 TG pattern of $Cu_2(NO_3)(OH)_3$

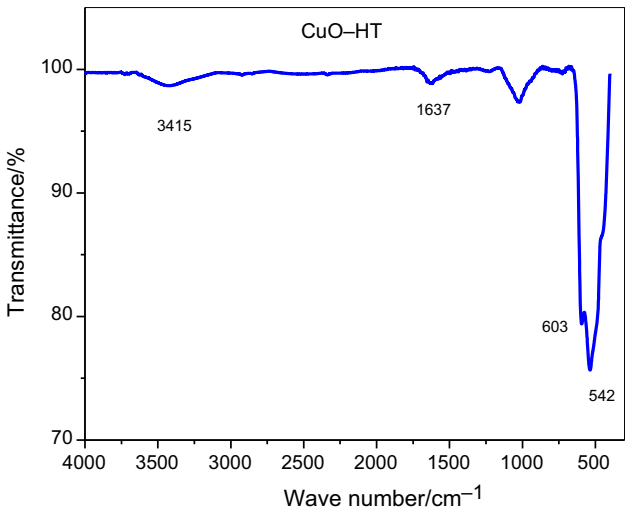

Fig. 3 FT-IR spectrum of CuO-HT

603 cm^{-1} and 542 cm^{-1} are attributed to the Cu–O stretching vibrations. The vibration peak at 3415 cm^{-1} indicates the presence of hydroxide group in sample. This is due to the water adsorbed on the surface of CuO. The metal oxygen bond is observed at 1637 cm^{-1} (M–O rocking out of plane) indicating the formation of CuO from copper nitrate.

The X-ray diffractogram of the CuO particles was recorded by using Cu Kα radiation. The XRD patterns of CuO particles prepared by hydrothermal method (CuO-HT) and direct decomposition method (CuO–C) are shown in Fig. 4. Peaks confirmed that CuO formed from both methods was in monoclinic phase. The characteristic peaks located at $2\theta = 32.58°$, 35.47°, 38.97° and 48. 74° are assigned to (110), (002), (200) and (202) plane orientation of CuO (PDF 04-007-1375).

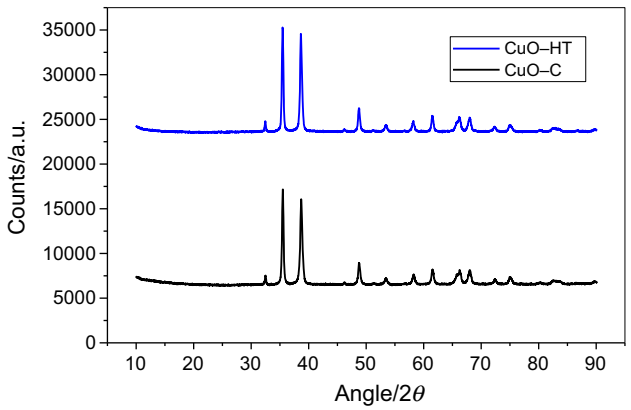

Fig. 4 XRD pattern of CuO prepared by different routes

The morphology and size of the prepared CuO particles were investigated by means of field emission scanning electron microscopy (FESEM). Figure 5a, b indicates the FESEM image of CuO–C and CuO-HT. As can be seen, sample CuO–C composed spherical agglomerate of flakes with each sphere diameter more than 10 μm, whereas CuO-HT sample possesses a flowerlike shape consisting of well-oriented petals which are fused at the bottom and spreads toward the top with sharp edges. This may be due to the slow formation and proper alignment of $Cu_2(OH)_3NO_3$ due to the slow and controlled change in pH throughout the solution in autoclave, which prevent the agglomeration of particles in the reaction chamber. Hierarchical pore structure of macro- and mesopores, evidenced from FESEM image, is advantageous for copper oxide particles to be acted as catalyst for AP decomposition.

The surface area and particle size of the samples were determined, and the specific surface area values calculated for each CuO samples are also listed in Table 1. Surface area and particle size analysis of CuO–C and CuO-HT confirmed that CuO-HT has low particle size (63.5 nm) and high specific surface area (17.3 $m^2\ g^{-1}$). CuO prepared by combustion method shows higher particle size (> 300 nm) and low surface area of 4.6 $m^2\ g^{-1}$ than that of CuO-HT.

The role of cotton in the hydrothermal reaction was further confirmed by conducting control experiments without cotton and found that reaction was not proceeded in the absence of cotton. Another trial was conducted using copper chloride salt as the starting material. Here also reaction was not successful due to the high decomposition temperature of chloride salt and the unavailability of oxidizing acidic species for cotton carbonization. Experiments were also conducted to optimize the amount of cotton required for the reaction. With excess cotton (> 2 mass%), most of the cotton remained partially carbonized along with the $Cu_2(OH)_3NO_3$ (Fig. 6).

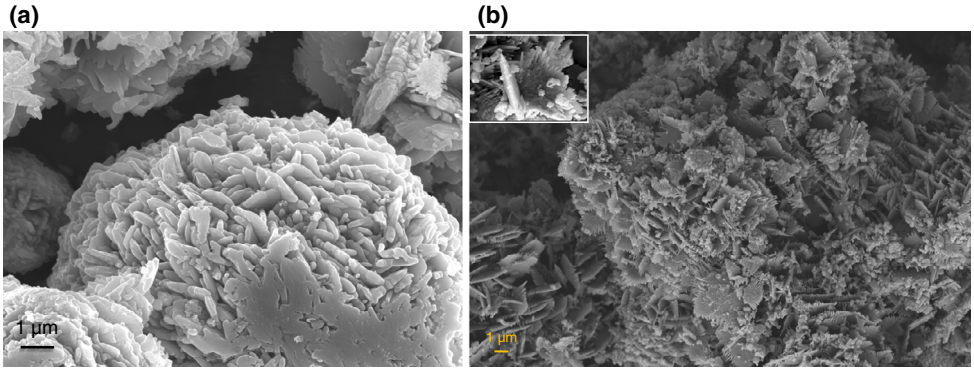

Fig. 5 FESEM analysis of **a** CuO–C and **b** CuO-HT

Table 1 Specific surface area and particle size of CuO powders

	Particle size/nm	Surface area/m^2 g^{-1}
CuO–C	> 300	4.6
CuO-HT	63.5	17.3

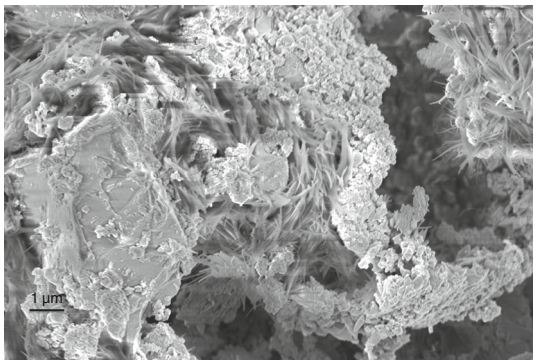

Fig. 6 FESEM image of $Cu_2(OH)_3NO_3$ formed in the presence of excess cotton

Effect of CuO on the thermal decomposition of ammonium perchlorate

Ammonium perchlorate shows low-temperature decomposition (LTD) below 300 °C and high-temperature decomposition (HTD) above 300 °C. Two mechanisms, viz, electron transfer mechanism and proton transfer mechanisms, were proposed as the decomposition mechanism of AP [21]. According to the proton transfer theory, proton transfer occurs from NH_4^+ to ClO_4^- during the initial decomposition of AP resulting in the formation of ammonia and perchloric acid. According to the electron transfer theory, AP decomposition is initiated by electron transfer from anion to cation which leads to $NH_4^{\cdot}$ and $ClO_4^{\cdot}$ species. Electron transfer theory is supported by the experimental evidences that the presence of electron mediators facilitates electron transfer from ClO_4^- to NH_4^+.

During the first stage of AP decomposition (below 300 °C), proton transfer mechanism is favored and gaseous intermediates, viz, ammonia and perchloric acid, are formed through partial dissociation as follows:

$$NH_4ClO_{4(s)} \leftrightarrow NH_4^+ + ClO_4^- \leftrightarrow NH_3(g) + HClO_4(g)$$

Some fraction of the evolved ammonia is oxidized by perchloric acid, and the remaining is adsorbed on the surface of un-decomposed AP particles. During the reactions occurring in the adsorbed layer, the perchloric acid is desorbed more rapidly than ammonia, which causes incomplete oxidation of ammonia, creating a saturated atmosphere of ammonia. The ammonia eventually covers the crystal surface to halt further reaction. When the surface of AP is covered by NH_3, it significantly retards the thermal decomposition of AP, and the decomposition ceases when 30% of AP decomposition happens. This retardation causes higher activation energies for the reaction to continue, and this has been observed in the case of the decompositions of AP [22]. As the temperature increases above 300 °C, the pre-adsorbed ammonia desorbs from the surface of AP and gas phase oxidation of ammonia with perchloric acid begins to take place with the formation of HCl, H_2O, N_2O, Cl_2, NO, O_2 and NO_2 [23].

Advantage of CuO as burn rate modifier is its unique property of changing into the stable fully filled 3d-orbital form of Cu^+ ($3d^{10}$) while mediating the electron transfer between NH_4^+ and ClO_4^- as per the following equations [24].

$$Cu^{2+} + ClO_4^- \rightarrow Cu^+ + ClO_4^{\cdot}$$

$$Cu^+ + NH_4^+ \rightarrow Cu^{2+} + NH_4^{\cdot}$$

It is reported that, in the presence of a transition metal oxide catalyst, electron transfer mechanism is favored for the thermal decomposition of AP [24–26]. Hence, quantity

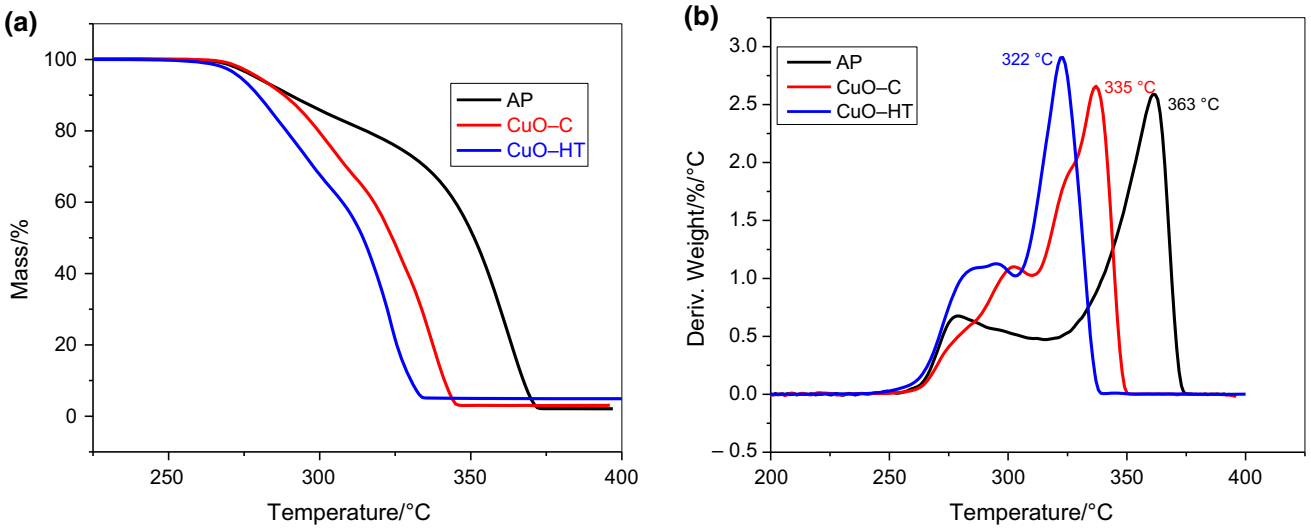

Fig. 7 TG (**a**) and DTG (**b**) of AP in the presence of 0.3% copper oxide

of un-oxidized ammonia and its further adsorption on AP surface is decreased. This can result in increased decomposition of AP in the presence of metal oxide burn rate modifier. The experimental evidence in terms of the quantity of gaseous products at the decomposition temperature of AP is lacking. In addition, CuO also accelerates the thermal decomposition of AP by the formation of less stable copper perchlorate intermediate. Figure 7a, b shows the TG and DTG plots, respectively, of AP decomposition with and without CuO catalyst. It can be seen that the T_1, the temperature of initiation of low-temperature decomposition (LTD) of AP, remains unaffected even in the presence of catalyst. Addition of 0.3% CuO–C and CuO-HT accelerates the thermal decomposition of AP by decreasing its overall decomposition temperature. From the DTG peaks (Fig. 7b), it is evident that the high-temperature thermal decomposition temperature (HTD) of AP is decreased from 363 to 335 °C and 322 °C for CuO–C and CuO-HT, respectively, i.e., the high-temperature decomposition of AP was decreased by 28 °C by CuO–C and 41 °C by CuO-HT. Thus, the catalytic activity of nanosized copper oxide (CuO-HT) is found to be better than that of microsized copper oxide (CuO–C).

Fine particle size and high surface area improve the mixing between the particles of the reactants and catalyst, thereby increasing the area of contact and more accessibility at the most reaction site. For a heterogeneous catalytic reaction like thermal decomposition of AP, these characteristics of catalyst are of prime importance. Even though the decomposition initiates inside the crystal lattice, the consumption of ammonia by perchloric acid/perchlorate species takes place at the surface of AP. Hence, the accessibility of burn rate modifier toward the critical reaction site is very much dependant on its particle size and surface area. Thus, maximum catalytic activity was showed by CuO-HT, due to its small size and higher surface area compared to all others. So, a good correlation between particle size/surface area and catalytic activity of copper oxide was observed here.

The decomposition mechanism of AP in the presence of nano copper oxide was further investigated by evolved gas analysis during AP decomposition. Type of gaseous products, their relative abundance and the temperatures at which gas evolution occurs were evaluated using thermogravimetry-mass spectrometer (TG-MS). Single ion chromatogram (SIC) for various volatile products obtained from TG-MS analysis of AP, AP + CuO–C and AP + CuO-HT during the thermal decomposition from 200 to 400 °C is shown in Figs. 8–9. TG-MS characterization of all compound/mixture indicates that AP decomposition reaction proceeds with the evolution of oxygen, nitrogen, nitrous oxide, nitric oxide, water, chlorine and ammonia.

The type of gases evolved at low temperature (< 300 °C) and high temperature (> 300 °C) was compared for AP, AP-CuO(C) and AP-CuO(HT) (Fig. 8). TG-MS analysis confirmed that NH_3 evolution has completed before 325 °C for AP + CuO-HT, which is low temperature compared to AP without catalyst. Thus, the evolved ammonia became more available for reaction with perchloric acid. MS analysis also confirmed the evolution of Cl_2, N_2 and O_2; the reaction products of ammonia and perchloric acid have shifted to lower temperature in the presence of CuO. The shift is more pronounced in the presence of nanosized CuO (CuO-HT), compared to the microsized CuO (CuO–C).

Figure 9 shows the amount of each species evolved for AP + CuO–C and AP + CuO-HT relative to those evolved in the case of AP without catalyst. Figure 9a–c

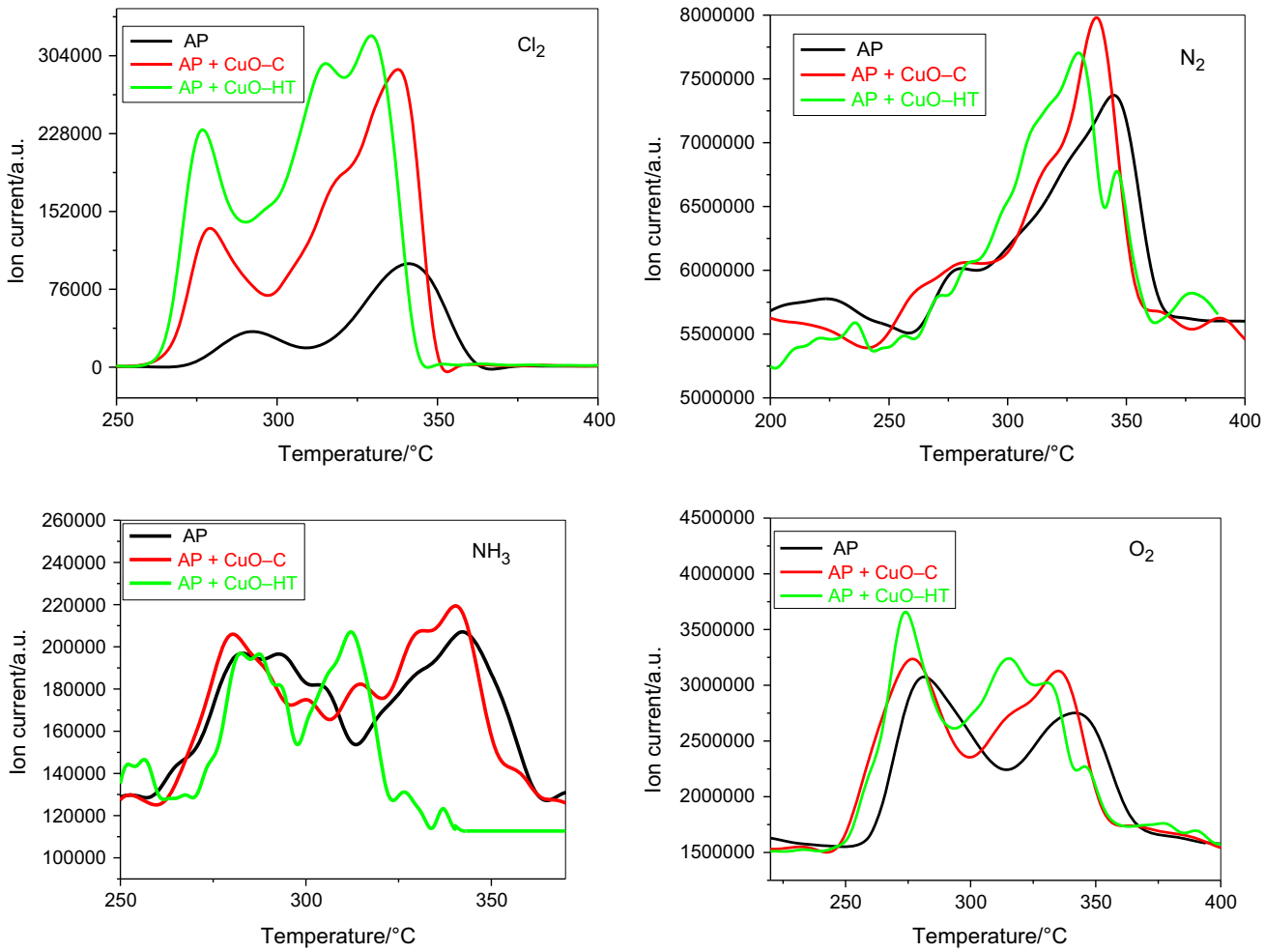

Fig. 8 Single ion chromatogram (SIC) of gas evolved during the decomposition of AP without and with catalyst at various temperatures

expresses the gas evolution at low-temperature (< 300 °C), high-temperature (> 300 °C) and whole (30–400 °C) decomposition regions, respectively. From Figs. 8–9, it can be seen that the type of volatile products from the thermal decomposition of AP with and without catalyst is almost similar for LTD and HTD. From TG-MS data, it is observed that in the presence of CuO the composition of volatile products drastically changed from LTD to HTD. N_2 and Cl_2 content increased in LTD, whereas O_2 and NO content increased in HTD. This indicates that in the presence of CuO, the decomposition mechanism of AP is different from that of pure AP decomposition. Figure 9c also indicates that O_2, NO, HCl and Cl_2 concentration in volatile products from catalyzed AP decomposition is higher than that of pure AP decomposition, whereas ammonia concentration is lower. Thus, from TG-MS data, it can be seen that oxidizing species like O_2, NO and Cl_2 are formed in the presence of CuO catalyst, which will accelerate the combustion of fuel in the propellant mix, thereby accelerating the burning rate. From the observations, it can be assumed that the proton transfer mechanism for the thermal decomposition of AP is switched over to electron transfer mechanism in the presence of copper (II) oxide, i.e., both catalyzed and uncatalyzed AP decomposition start with proton transfer mechanism indicated by the evolution of ammonia. But, copper (II) oxide favors the electron transfer mechanism by acting as mediator for electron transfer. This will reduce the formation of ammonia and increase the oxidation of ammonia by the decomposition products of perchlorate species.

To further confirm the above-proposed mechanism, nitrogen evolution was studied for AP decomposition. As expected, the amount of nitrogen evolved for AP + CuO-HT is almost double that of AP alone. Since N_2 is the oxidation product of ammonia, the result agrees the interpretation that ammonia reacts with perchlorate to the maximum extending at lower temperature itself. The amount of free ammonia evolved has also reduced

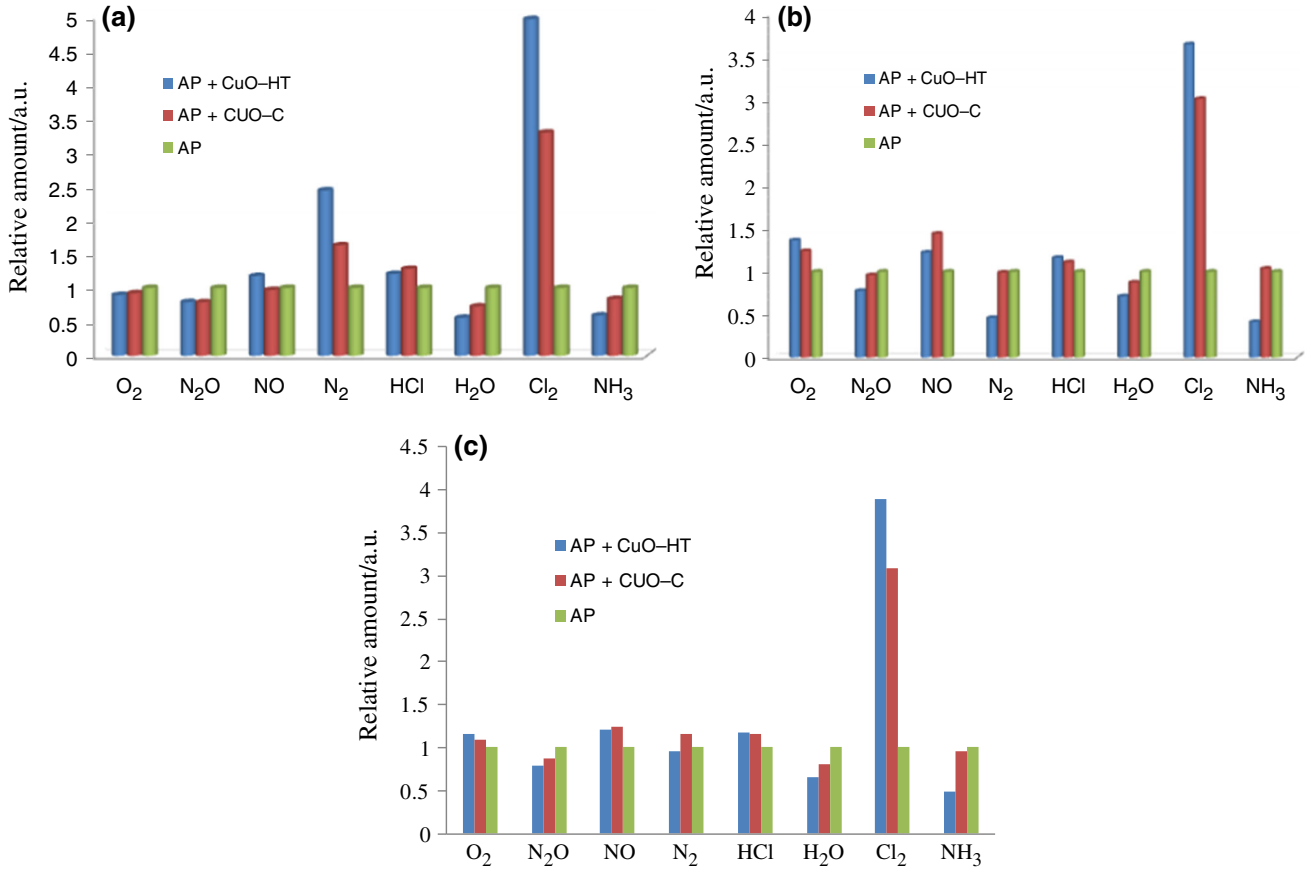

Fig. 9 Comparison of relative amount of gas evolved during the thermal decomposition of AP without and with catalyst

throughout the whole process, due to the catalyst-enhanced oxidation. All these observations show a linear trend for nanosized CuO and microsized CuO, confirming that the change in AP decomposition pattern is solely due to the influence of CuO, whose catalytic activity depends on the surface area, particle size and, thus, the number of active sites.

Conclusions

Nano copper oxide burn rate modifiers were prepared by hydrothermal reaction without the use of alkali or shape-controlling agents. Addition of small amount of cotton acted as pH-controlling agent through its hydrothermal carbonization, by utilizing the nitric acid produced from copper nitrate. Well-defined nanosized particles with open pores were confirmed by FESEM analysis. Significance of hydrothermal reaction confirmed by comparing its property with that of CuO prepared through combustion method. Due to the high surface area and low particle size in nanorange, CuO prepared by hydrothermal method performed as a better catalyst for the thermal decomposition of ammonium perchlorate. TG-MS data of volatile products of decomposition of AP showed increased concentration of N_2, Cl_2, O_2 and a reduced concentration of ammonia. This indicates a change in mechanism of decomposition of AP from proton transfer mechanism (for pure AP) to electron transfer mechanism of Cu(II)O catalyzed AP. This work provided insight into the catalytic mechanism of CuO for AP decomposition.

Acknowledgements Authors acknowledge Director, VSSC, for the fund.

References

1. Boldyrev VV. Thermal decomposition of ammonium perchlorate. Thermochim Acta. 2006;443:1–36.
2. Kishore K, Sunitha MR. Effect of transition metal oxides on decomposition and deflagration of composite solid propellant systems. AIAAJ. 1979;17:1118–25.
3. Juibari NM, Tarighi S. $MnCo_2O_4$ nanoparticles with excellent catalytic activity in thermal decomposition of ammonium perchlorate. J Therm Anal Calorim. 2018;133:1317–26.
4. Pandas HM, Fazli M. Fabrication of MgO and ZnO nanoparticles by the aid of eggshell bioactive membrane and exploring their catalytic activities on thermal decomposition of ammonium perchlorate. J Therm Anal Calorim. 2018;131:2913–24.

5. Hosseini SG, Ayoman E. Synthesis of α-Fe_2O_3 nanoparticles by dry high-energy ball-milling method and investigation of their catalytic activity. J Therm Anal Calorim. 2017;128:915–24.
6. Pearson GS. The role of catalysts in the ignition and combustion of solid propellants. Combust Flame. 1970;14(73–84):19.
7. Chaturvedi S, Dave PN. Nano-metal oxide: potential catalyst on thermal decomposition of ammonium perchlorate. J Exp Nanosci. 2012;7:205–31.
8. Patil PR, Krishnamurthy VE, Joshi SS. Effect of Nano-copper Oxide and Copper Chromite on the Thermal Decomposition of Ammonium Perchlorate. Propellants Explos Pyrotech. 2008;33:266–70.
9. Mahdavi M, Farrokhpour H, Tahriri M. Investigation of simultaneous formation of nano-sized CuO and ZnO on the thermal decomposition of ammonium perchlorate for composite solid propellants. J Therm Anal Calorim. 2018;132:879–93.
10. Ayoman E, Hosseini SG. Synthesis of CuO nanopowders by high-energy ball-milling method and investigation of their catalytic activity on thermal decomposition of ammonium perchlorate particles. J Therm Anal Calorim. 2016;123:1213–24.
11. Zheng L, Liu X. Solution-phase synthesis of CuO hierarchical nanosheets at near-neutral pH and near-room temperature. Mater Lett. 2007;61:2222–6.
12. Lugo-Ruelas M, Amezaga-Madrid P, Esquivel-Pereyra O, Antúnez-Flores W, Piza-Ruiz P, Ornelas-Gutierrez C, Miki-Yoshida M. Synthesis, microstructural characterization and optical properties of CuO nanorods and nanowires obtained by aerosol assisted CVD. J Alloys Compd. 2015;643:S46–50.
13. Tadjarodi A, Roshani R, Imani MA. Facile and green synthesis of CuO nanowires by mechanochemical method. ChemXpress. 2014;6:25–9.
14. Wu S, Li F, Zhang L, Li Z. Enhanced field emission properties of CuO nanoribbons decorated with Ag nanoparticles. Mater Lett. 2016;171:220–3.
15. Bhuvaneshwari S, Gopalakrishnan N. Enhanced ammonia sensing characteristics of Cr doped CuO nanoboats. J Alloy Compd. 2016;654:202–8.
16. Yang C, Xiao F, Wang J, Su X. 3D flower- and 2D sheet-like CuO nanostructures: microwave-assisted synthesis and application in gas sensors. Sens Actuators B. 2015;207:177–85.
17. Ba N, Zhu L, Zhang G, Li J, Li H. Facile synthesis of 3D CuO nanowire bundle and its excellent gas sensing and electrochemical sensing properties. Sens Actuators B. 2016;227:142–8.
18. Ameri B, Saeed S, Davarani H, Roshani R, Moazami HR, Tadjarodi A. A flexible mechanochemical route for the synthesis of copper oxide nanorods/nanoparticles/nanowires for supercapacitor applications—the effect of morphology on the charge storage ability. Jalcom. 2017;695:114–23.
19. Paulose S, Rajeev R, George BK. Functionalized white graphene—copper oxide nanocomposite: synthesis, characterization and application as catalyst for thermal decomposition of ammonium perchlorate. J Colloid Interface Sci. 2017;494:64–73.
20. Sun P, Wang S, Zhang T, Li Y, Guo Y. Supercritical hydrothermal synthesis of submicron copper(II) oxide: effect of reaction conditions. Ind Eng Chem Res. 2017;56:6286–94.
21. Jacobs PWM, Pearson GS. Mechanism of the decomposition of ammonium perchlorate. Combust Flame. 1969;13:419–30.
22. Vyazovkin S, Wight CA. Kinetics of thermal decomposition of cubic ammonium perchlorate. Chem Mater. 1999;11:3386–93.
23. Devi TG, Kannan MP, Hema B. Thermal decomposition of cubic ammonium perchlorate—the effect of barium doping. Thermochim Acta. 1996;285:269–76.
24. Chaturvedi S, Dave PJ. A review on the use of nanometals as catalysts for the thermal decomposition of ammonium perchlorate. Saudi Chem Soc. 2013;17:135–49.
25. Eslami A, Juibari MM, Hosseini SG. Fabrication of ammonium perchlorate/copper-chromium oxides core-shell nanocomposites for catalytic thermal decomposition of ammonium perchlorate. Mater Chem Phys. 2016;181:12–20.
26. Joshi SS, Patil PR, Krishnamurthy VN. Thermal decomposition of ammonium perchlorate in the presence of nanosized ferric oxide. Def Sci J. 2008;58(271–272):11.